Scientia Iranica A (2015) 22(3), 679–698

SCIENTIA IRANICA

Sharif University of Technology
Scientia Iranica
Transactions A: Civil Engineering
www.scientiairanica.com

Measuring wave velocity, damping and stress-strain behaviors of geo-materials using GAP-SENSOR

A. Aghaei Araei[a,*], I. Towhata[b], H.R. Razeghi[c] and S. Hashemi Tabatabaei[a]

a. *Department of Geotechnical Engineering, Road, Housing and Urban Development (BHRC), Tehran, P.O. Box 13145-1696, Iran.*
b. *Geotechnical Engineering Group, Department of Civil Engineering, University of Tokyo, 7-3-1 Hongo Bunkyo-ku, Tokyo, P.O. Box 113-8656, Japan.*
c. *School of Civil Engineering, Iran University of Science and Technology (IUST), Tehran, P.O. Box 16765-163, Iran.*

Received 15 January 2014; received in revised form 13 July 2014; accepted 6 December 2014

KEYWORDS
Wave velocity;
Modulus;
Damping;
Monotonic;
Dacite;
Mudstone;
Tire chips;
Toyoura.

Abstract. A triaxial testing system is described for measuring the wave velocity, stiffness, damping and stress-strain behavior of layered granular materials and rock specimens under impact, cyclic and monotonic loading. The system is equipped with high-frequency GAP-SENSORs (GSs) in front of target plates connected on the side of a specimen surface to measure wave velocity, axial and radial deformations locally, LDTs to measure axial and radial deformations locally, and a load cell. Based on the first arrival of compressional wave of the deformation time-histories under impact loading, the pulse velocity is evaluated. In addition, using a reduced deformation amplitude technique at different elevations of the specimen, damping ratio is calculated. Results indicate that measurement of the wave velocity and damping ratio using low noise level GSs is a simple, nondestructive and reproducible method. Comparing the results of small strain shear modulus and damping ratio using local axial and radial strains measured by LDTs and GSs in the cyclic loading, with those of the proposed method, the high precision of the used innovative method is confirmed. Using this system, a continuous stress-strain relation for a strain range of 0.0001% to several % can be obtained from a single test using a single specimen.

1. Introduction

Recently, usage of lightweight rockfill material and even lightweight soil has been proposed to reduce lateral earth pressure [1]. In addition, granulated pure tire rubber and soil-rubber mixtures have been used as backfill material in retaining walls and buried pipes (to reduce the lateral earth pressures) as construction material in embankments overlying soft or unstable soils (to reduce the vertical stresses and settlements), or as an isolation system (to modify the seismic response of foundations/superstructures) [2,3]. There are many uncertainties about the behavior of lightweight rockfill, granular soil/ rubber tire chip mixtures and layered soil (i.e. ballast and sub-ballast in rail tracks, filters) under monotonic, cyclic and dynamic loading conditions at low confining pressure. Testing the representative samples using suitable field or laboratory equipment is an essential prerequisite to determine the realistic behavior of materials.

The most important dynamic parameters of soils and rockfill in any dynamic analysis are the maximum shear modulus ($G_{\max}$), shear modulus (G) and damping ratio (D). Many researchers have investigated factors that may affect these parameters [4-11]. These factors are: confining pressure, strain history,

*. *Corresponding author. Tel.: +98 21 88255942; Fax: +98 21 88255942*
E-mail addresses: aghaeiaraei@bhrc.ac.ir (A. Aghaei Araei); towhata@geot.t.u-tokyo.ac.jp (I. Towhata); rezeghi@iust.ac.ir (H.R. Razeghi); htabatabaei@bhrc.ac (S. Hashemi Tabatabaei)

disturbance (geological age, cementation), fine grain percentage, gravel percentage, number of cycles, strain level, relative density, loading frequency, waveform, moisture, drainage conditions, anisotropy, soil type, grain shape, plasticity index and even the type of testing machine. In soil-rubber mixtures, the main factors to strongly affect their behavior are the amounts of rubber, particle size, shape, and mass density of rubber solids they contain, as well as the dynamic properties of the soil. Moreover, the predominant behavior that the mixtures exhibit, the soil-like or tire chip-like behavior, depends on the predominant interfaces of the soil-tire chips solid skeleton [12-14].

Generally, the effect of loading frequency at small strain is important. However, due to the nonlinear behavior at large strain, the number of cycles and volume change behaviors may become important as well. Laboratory tests to determine the soil and rock properties at small strains are as follows: resonant column test (for soil) [15-17], ultrasonic test (for soil and rock) [18-20], and piezoelectric bender elements for S-wave generation using a cantilever type or P-waves by piezoelectric disks for the soil [21-23]. Various potential sources of error and difficulties in the aforementioned testing systems have been cited in the literature. The crucial point is the difference between measured values of maximum shear modulus and damping ratio between different testing equipment [15].

In recent years, using advanced triaxial apparatus for simultaneous recording of the stress-strain of geomaterials has become very popular. In this system, the deviator load has been measured by a load cell placed directly above the specimen top cap inside the triaxial cell. Moreover, local axial strains free from bedding errors have been measured by a pair of Local Deformation Transducers (LDTs) [24] hinged vertically on the sides of the specimen surface, and the local lateral strains of an unsaturated specimen have been measured using three pairs of gap sensor or clip gauge [25] at three levels of specimen height. Generally, for tests at a constant effective confining pressure, errors involved in the lateral strain measured by these methods should be small [26]. A comprehensive and comparative study on local deformation transducers has been published by Scholey et al. [27]. In addition, wave velocity has been measured by accelerometers [28] in the triaxial specimen. Besides, the GS has been used to measure the displacement of the loading cap (i.e. conventional axial strain measurement) of triaxial apparatus [29]. Axial strains evaluated by GSs might be affected by system compliance and bedding error [30]. Moreover, in the case of rockfill specimens, the shear slippage of LDT over membranes with thicknesses higher than 2 mm, employing the extrapolation method from 0.0001% strain to obtain $G_{\max}$ in the case of LDT and GS [4], high noise level and, as a result, difficulty in determination of travel time for accelerometers, are examples of the deficiency of the equipment.

It seems that there is no published paper dealing with the use of GSs for simultaneous measurement of wave velocity, Poisson's ratio, damping ratio under impact loading and then cyclic loading. This study looks at these issues, as well as comparing the results of GSs with those of other measurements, such as LDTs, on the different geo-materials, via large cyclic triaxial and uniaxial testing systems.

2. Testing systems specifications

Experimental work, including monotonic, pulse velocity and cyclic testing, is conducted using large (30 cm diameter) and small (10 cm diameter) triaxial apparatus at the Geotechnical Laboratory in the Department of Civil Engineering at Tokyo University, Japan. There are automated gear-clutch loading systems driven by an AC-servo motor [31]. This equipment is able to shear specimens in stress or strain control modes. A rubber head hammer, being about 2.2 kg in weight, was used to hit (impulse) the rod connected to the top cap of the specimen in a vertical direction (Figure 1). Cell

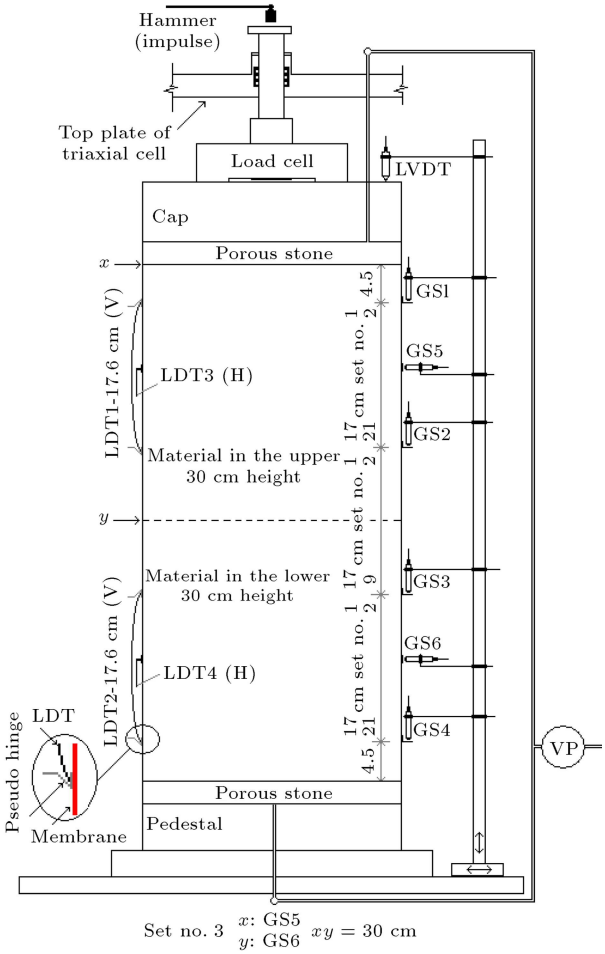

Figure 1. The triaxial apparatus.

Table 1. Characteristics and calibration factors of the used sensors.

Sensor type	Sensor no./serial number	Displacement (mm), load (ton), pressure (kPa) =(A=?)Volt, R2	Amplifier setting	Maximum capacity
Load cell-MLC		1.803,0.999	ATT: 1/20, filter: 30 Hz, Cal: 5000 ($\mu\varepsilon$)	70 kN
LVDT-DTH-A-10	EK143004	0.480, 1.000	ATT: 1/5, filter: 30 Hz, Cal: 3000 ($\mu\varepsilon$)	10 mm
Lateral or back pressure transducer, Kyowa Type PGM: 10 K H	ED64600018	0.467, 0.999	ATT: 1/10, filter: 10 Hz, Cal: 2000 ($\mu\varepsilon$)	1000 kPa
LDT1-vertical displacement	Top1	-0.0163v^2+0.0062v+ 23.326, 1.000	ATT: 1/5, filter: 30 Hz, Cal: 3000 ($\mu\varepsilon$)	2.5 mm
LDT2-vertical displacement	Bottom2	-0.0779v^2+0.0276v+ 23.156, 1.000	ATT: 1/5, filter: 30 Hz, Cal: 3000 ($\mu\varepsilon$)	2.5 mm
LDT3-cantilever type-horizontal deformation	Top3	0.0019v^2-0.02075v+ 8.9837, 0.999	ATT: 1/10, filter: 30 Hz, Cal: 3000 ($\mu\varepsilon$)	1.5 mm
LDT4-cantilever type-horizontal deformation	Bottom4	0.002v^2 - 0.2639v + 6.1919, 0.999	ATT: 1/5, filter: 30 Hz, Cal: 3000 ($\mu\varepsilon$)	1.5 mm
GAP-SENSOR	1-12188	0.495, 0.998	—	$4-6^a$ mm
GAP-SENSOR	2-12192	0.556, 0.993	—	$4-6^a$ mm
GAP-SENSOR	3-12186	0.362, 0.994	—	$4-6^a$ mm
GAP-SENSOR	4-12187	0.445, 0.997	—	$4-6^a$ mm
GAP-SENSOR	5-12189	0.474, 0.997	—	$4-6^a$ mm
GAP-SENSOR	6-12185	0.464, 0.999	—	$4-6^a$ mm

[a]: For galvanized target plate.

pressure was supplied by applying a vacuum inside the specimen. A diaphragm type pressure transducer was used for the vacuum measurement inside the specimen. Table 1 presents the characteristics and calibration factors of the used sensors. A Linear Variable Displacement Transducer (LVDT), as well as two LDTs (176 mm in height), were used for measurement of axial deformation. Moreover, two sets of cantilever type LDTs were used for the measurement of radial deformations (Table 1). All the above transducers were connected to a data acquisition system through a single-channel carrier frequency amplifier. The data acquisition system (DRA 30A, TML company) has thirty independent channels and are used under monotonic and cyclic loading conditions. It can record data for an interval of less than 0.1 msec.

Due to the special characteristics of the non-contacting displacement measuring system or Gap-Sensors (GSs), they were used as a non-contacting displacement measuring system, as well as for pulse velocity measurement. The latter is based on the first arrival of the compressional wave of deformation time-histories under impact loading. Six sets of GS were used for measuring wave velocity, and axial and lateral deformation in this study.

Generally, GS is called "an eddy current displacement sensor". A high-frequency current is supplied to the coil inside the sensor head to generate a high-frequency electromagnetic field. When the target (a conductive or magnetic substance) approaches this electromagnetic field, an eddy current is generated on the surface of the target and the sensor coil impedance is changed. The sensor system detects the change in oscillation strength resulting from this phenomenon to identify the relationship between displacement and voltage.

System components include: Sensor model, PU09, with gap measuring range of 0-4 mm (6 mm for galvanized iron) and a resolution of 0.3 μm, cable, PC-03YY, adopted converters, AEC 5509, and amplifier. The response frequency of converters for the DC power supply is 30 kHz, which is ten times higher than that of the available accelerometer for measuring wave velocity. Moreover, the common type of PU09 has 65 MPa static resistance against air pressure.

The GS in front of the target plate at a distance of

2 mm is connected to the converter and the output of the amplifier is recorded by data acquisition. Moreover, the AC power is changed to DC power by 55SPS-3 to be connected to the amplifier. This system is manufactured by the Applied Electronics Corporation (AEC). An eight-channel recording device, ZR-MDR10, manufactured by OMRON Company, Japan, was used to record the GSs results at different elevations and locations under impact loading. This data acquisition uses ZR-SV10 software and has a 100 kHz sampling rate for each channel for a maximum period of 10 seconds.

Figure 1 shows the used large triaxial apparatus configuration, as well as a schematic diagram of the place to be hit to produce the impulse. More details about the triaxial and uniaxial equipment, sensor arrangement around the specimens, and calibrations are presented in [8,9].

3. Materials properties

The materials under study are tire chips, Toyoura sand, angular granulated lightweight mudstone from the Yokosuka site, and sand and gravel angular Dacite (lapilli and ash) from the Unzen Volcano in Japan. The gradation curves of the used materials are shown in Figure 2. The maximum particle size of the tested materials is 19 mm.

Tables 2 and 3 summarize the main characteristics

Table 2. Results of G_s for the materials.

Materials (particle size)	G_s
Mudstone (0.25 mm-19 mm)	2.22
Mudstone (9.5 mm-19 mm)	1.85
Mudstone (9.5 mm-19 mm)	2.40
Dacite (9.5 mm-19 mm)	2.35
Toyoura sand	2.65
Tire chips [32]	1.17

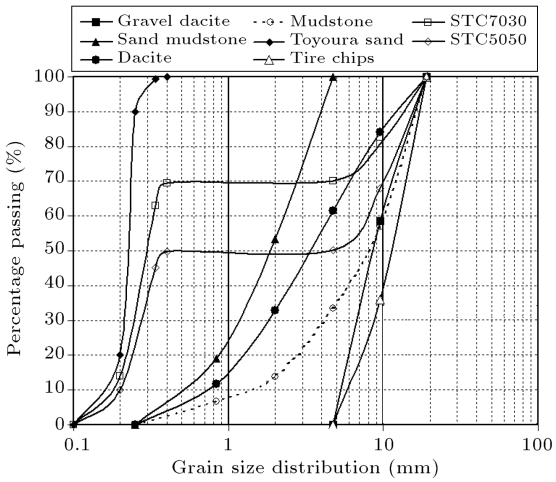

Figure 2. Gradations of the tested materials.

of the materials, including specific gravity and ranges of particle size/dry density, respectively. Specific gravity was estimated for samples, according to ASTM C127 [33], which were used for determination of the initial void ratio. Results of Table 2 indicated that specific gravity (Gs) decreases as particle size increases, due to the extra void space in the bigger rockfill particle. The Gs of sand is two times higher than of tire chip. It is found that the tire chip Gs value (1.17) lies between the ranges (1.02-1.27), as proposed by previous researchers [14].

Maximum dry density, $\gamma_{d\max}$, was estimated for the sample, according to Standard Proctor [34]. Compared to conventional soil material, like sand and gravel, tire chips are considered a lightweight material; $\gamma_{d\max}$ = 500-900 kN/m^3, depending on compaction and overlaying pressure [35]. Maximum dry density of tire chips is one-third of Toyoura sand. Moreover, for the purpose of brevity, the names of the materials are introduced with their abbreviations (Table 3). The Los Angeles abrasion test was conducted according to [36]. This test has been widely used as an indicator of the relative quality or competence of various sources of

Table 3. Results of dry density test for the materials.

Materials (particle size)	**Material symbol**	γ_d **(kN/m^3)**
Mudstone (0.25 mm-19 mm)	1	11.75
Mudstone-gravel (4.75 mm-19 mm)	2	10.00
Mudstone-sand (0.25 mm-4.75 mm)	3	10.00
Dacite (0.25 mm-19 mm)	4	16.50
Dacite-gravel (4.75 mm-19 mm)	5	14.38
Dacite-sand (0.25 mm-4.75 mm)	6	15.56
Toyoura sand (0.1 mm-0.4 mm)	7	6,74
Tire chips (9.5 mm-19 mm) [32]	8	6.74
Toyoura sand 50%+ Tire chips 50% (0.1 mm - 19 mm)	9	11.66
Toyoura sand 70%+ Tire chips 30% (0.1 mm - 19 mm)	10	14.63

aggregate having similar mineral compositions. The value was about 45.6% and 5.4% after 1000 revolutions for Mudstone and Dacite, respectively.

4. Experimental programs

Several layered specimens were prepared and tested under different low confining pressure conditions, in order to study the granular soils (i.e. Mudstone, Dacite, Tire Chips, Toyoura sand) and their mixture properties, especially at interface locations. These tests were conducted on large scale specimens, 30 cm in diameter and 60cm in height, using large-scale triaxial equipment. Table 4 presents material symbols, material type in the upper or lower 30 cm in the layered specimen with 60 cm height, as well as different tests and their procedures. Over 108 wave velocity, Poisson ratio and damping ratio tests were carried out at isotropic confining pressures of 30, 50 and 80 kPa under impact loading at small strain. Generally, many measurements may be made on the same specimen with various states of ambient shearing strain levels of less than 0.01% [16,37]. Therefore, on the same specimens (used for impulse loading), cyclic or monotonic tests were performed. The cyclic triaxial tests were carried out in this research at a confining pressure of 50 kPa, according to ASTM D3999 [37]. Moreover, monotonic tests at an isotropic confining pressure of 50 kPa, according to ASTM D4767 [38], were performed in this research (Table 4). The wave velocity, monotonic and cyclic tests over the intake and cracked Mudstone rock specimen, were also carried out under uniaxial conditions, using the small (10 cm diameter and 20 cm height) triaxial equipment.

4.1. Preparation of granular specimens

For each triaxial specimen, the weight proportion of various grain sizes, required to achieve the granular material grain size distributions, were determined by weight. A silicone type membrane with a thickness of 2.5 mm, complying with ASTM D3999 [37] and ASTM D4767 [38], was used to encase the specimen. The Young's modulus (E_m) of the used membrane is 750 kPa. Increase of deviator stress for ε_1=15% (0.15 in decimal form) is less than 4 kPa. We ignore the membrane correction effect over the measured deviator stress. A vacuum was supplied to the split mold to pull the membrane against its side and hold it tightly

Table 4. Characteristics of materials and testing programs.

Specimen symbol	Material in 30 cm (symbol Table 3)		Sensor set up (Figure 1)	Testing programs
	Upper	Lower		
M02519GS	2	3	1	A and B
M02519GS	2	3	1	A and B under anisotropic condition ($\sigma_1'/\sigma_3'=2$)
D02519GS	5	6	1	A and B
M0219	1-fresh	1-reused	1	A and B
D0219	4-fresh	4-reused	1	A and B
MD0219	1	4	1	A and B
DM0219	4	1	1	A and B
MD0219-fresh	1	4	1	A and B
STC	7	8	1	A and B
STC	7	8	1	C
STC5050-7030	9(STC5050)	10(STC7030)	1	A and B
STC5050-7030	9(STC5050)	10(STC7030)	1	C
MONO-MD0219	1	4	2,3	D and C
MONO-D02519GS	5	6	2,3	D and C
MONO-M02519GS	2	3	2,3	D and C

Legend:

A: Wave velocity and damping ratio measurements at isotropic confining pressures of 30, 50 and 80 kPa with three times repetition under impulse loading.

B: Cyclic triaxial test according to ASTM D 3999 under isotropic confining pressure of 50 kPa (after A).

C: Monotonic test according to ASTM D 4767 (after A or D).

D: Wave velocity and damping ratio measurements, focusing on the interface and thickness effects for different sensors arrangement.

during the compaction operation. The specimens were prepared to the desired dry density, according to ASTM D698 [35], in a split mold, using a wooden weight of 5.2 kg. Specimens were constituted in six layers.

After compacting the last layers, the vacuum was removed over the mold and an inside vacuum of around 15-25 kPa was applied to the specimen. Then, the split mold was opened and specimens were first subjected to the required confining pressure via applying suction [21]. At the end of this stage, different measuring systems for measuring wave velocity and local strains were mounted over the side of the specimen.

4.2. Monotonic loading triaxial tests

Monotonic triaxial compression tests were used to study the stress-strain-strength behavior of the different granular materials. Five monotonic Consolidated Drained (CD) triaxial tests were performed after impulse loading at an isotropic confining pressure of 50 kPa on the dry specimens (Table 4). All monotonic tests were performed using a strain-controlled compression loading system. Different measurements, including GS, LDT and LVDT, were used for axial and lateral deformation measuring. After applying the confining pressure, the axial load was applied up to axial strain to about 17%. For GSs transducers, due to limitations of the measuring range (6 mm) and the need for large strain, several adjustments to the target plate were undertaken during testing. The imposed axial strain rate was 0.5% per minute. During the test, the amount of axial stress, and axial and radial strains were recorded at different places on the side of the specimen (mixture).

4.2.1. Presentation of the results

Table 5 presents a summary of the results of monotonic triaxial tests, including maximum deviator stress ($q_{\max}$) and effective internal friction angle at maximum deviator stress (ϕ'). Previous studies on pure tire chips indicate that triaxial tests give a zero cohesion intercept for confining pressures of less than 55 kPa, while the tests performed at confining pressures higher than 82 kPa, show cohesion [10]. Moreover, maximum friction angles for used sand and gravel are calculated for each single confining pressure, assuming $c = 0$, and using the following equation:

$$\sin\phi' = \left(\frac{\sigma'_1 - \sigma'_3}{\sigma'_1 + \sigma'_3}\right)_{\max}. \quad (1)$$

Generally, the internal friction angle of the materials under study range between $31.6° - 49.2°$ for the confining pressure of 50 kPa. Stress-axial strain-radial strain behaviors of tested specimens subjected to monotonic loading are shown in Figure 3. Figure 3(a) indicates that the lightweight M02519GS specimen shows slightly higher maximum deviator stress, corresponding to higher axial strain, in comparison to the D02519GS specimen. It seems that STC and pure tire chip materials, respectively, have the lowest maximum deviator stress between the tested specimens and materials. The STC7030 shows stiffer behavior in comparison to STC5050 and pure Toyoura sand. Moreover, axial strain in the middle part of the specimens is higher than that of the total length of the specimens (Figure 3(b), (c) and (d)). In some specimens, including STC and STC 5050, due to sand fall and segregation at the place of the target plate of GSs on the side of the specimen, the negative values of axial deformation were measured (Figure 3(c) and (e)). However, this behavior was not observed when using LVDT at the top of the specimen (Figure 3(a)). Therefore, assessment of the self-motion behavior and local segregation of granular materials are advantages of using GS. Moreover, the stress-axial strain behaviors using LDTs (Figure 3(f)) are in good agreement with GS results (Figure 3(d)). Results presented in Figure 3(h) indicated that the radial strain of gravel is higher than that of the sand, and all the materials show dilation trends in their radial strain behavior. Moreover, the radial strain using LDTs is in good agreement with GS results (Figure 3(g) and (h)).

4.2.2. Stiffness for primary loading

The stress-strain behaviors for primary loading in triaxial tests are highly nonlinear. Parameter E_{50}, which is used for defining a standard drained triaxial

Table 5. Summary of monotonic triaxial tests results.

Specimen symbol	$q_{\max}$ (kPa)	ϕ' (Peak)	E_{50} (kPa) (LDT)	E_{50} (kPa) (GSs distance=51 cm)	E_{50} (kPa) (GSs distance=9 cm)	E_{50} (kPa) for material in the upper 30 cm / lower 30 cm (GS)
STC	110	31.6	2176	2973	2821	14474/1677
STC5050-7030	168	38.8	4057	15000	11667	20488/15000
D02519GS	259	46.2	23214	33333	14130	86667/28889
M02519GS	278	47.3	14000	18667	8333	24561/26415
MD0219	311	49.2	14486	22059	10000	19277/50000

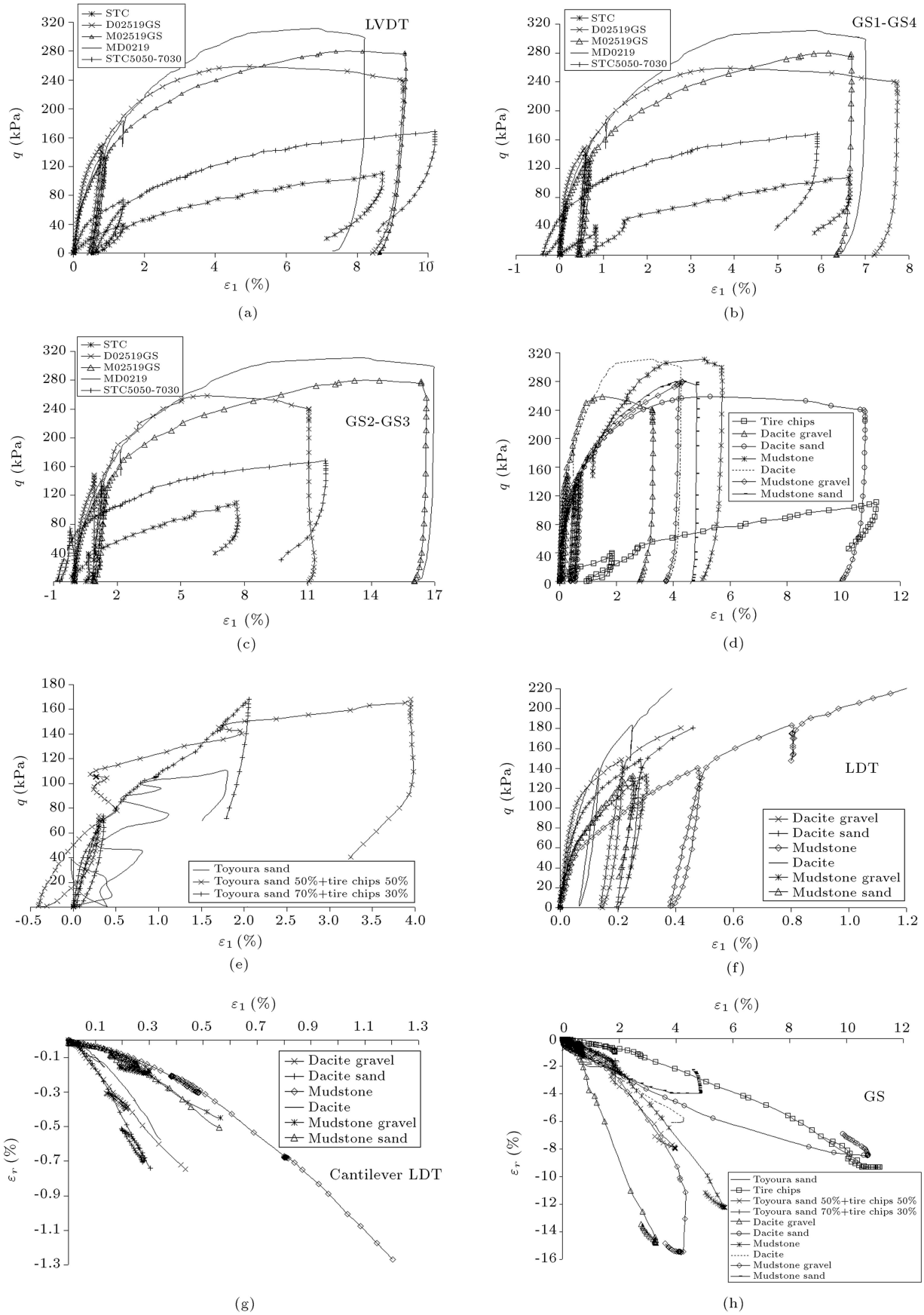

Figure 3. Stress-radial, strain-axial and strain relationships of the granulate materials using large triaxial equipment.

test curve, is the confining stress dependent stiffness modulus for primary loading. The secant modulus (E_{50}) is used instead of the tangential modulus (E_i) for small strain, which is more difficult to determine experimentally. The secant modulus, E_{50}, is determined from the triaxial stress-strain curve for mobilization of 50% of maximum shear strength. The actual stiffness depends on the minor principal stress, σ'_3, which is the effective confining pressure in a triaxial test. For confining pressure of 50 kPa, the range of the secant modulus is between 2176 and 33333 kPa (Table 5), for specimens 60 cm in height. Moreover, the range of E_{50} (kPa) of the material in the upper 30 cm and lower 30 cm using GS, is between 1677 and 86667 kPa.

4.3. Evaluation of shear wave velocity using impact loading

Elastic wave propagation measurements have been used in many field and laboratory geotechnical testing apparatuses to examine the small shear strain stiffness of soil and rock. There have been few efforts, thus far, to measure the P-wave velocity in laboratory soil samples because of the lack of recognition of its importance in engineering application. The measurements of the P-wave do not induce any disturbance to intact soil, neither in the field nor in the laboratory, because the induced shear strain is infinitesimally small (non-destructive test). Thus, the monotonic and cyclic tests performed after P-wave measurements are completely free from the effects of sample disturbance [39].

Using high frequency GS for the measurement of wave velocity required setting them up at different levels in horizontal and vertical directions, in front of target plates attached to the membrane or the lateral sides of specimen surfaces. The performance of GSs on specimen surfaces could eliminate system compliance and bedding error. According to Santamarina et al. [40,41], the impact can be used as the source of small impulsive elastic waves. P-wave velocity (V_p) is calculated directly by measuring the travel distance (L) and travel time (T) from the recorded deformation time-history, using GSs data:

$$V_p = L/T. \tag{2}$$

The V_p is proportional to the soil constraint modulus, M, and is expressed as:

$$M = \rho.V_p^2, \tag{3}$$

where ρ is the bulk mass density of the soil. The M and Young modulus, E, are related to each other by the following equation:

$$M = E\left[(1 - v_{\text{ske}})/(1 + v_{\text{ske}})(1 - 2v_{\text{ske}})\right], \tag{4}$$

where v_{ske} is the Poisson ratio of the soil skeleton, which is assumed to take a constant value, irrespective of relative density and confining pressure [39]. Moreover, by measuring horizontal and vertical strains using GS, the overall Poisson ratio, v, can be calculated. Thus, the small shear modulus (G) can be calculated as:

$$G = \frac{E}{2(1 + v)}, \tag{5}$$

when the impact is applied to the top cap of the specimen, it is observed that the waveform changes its shape at about 550 mm away and wave interference is induced. Generally, wave generation by impact causes point source vibration, forming a spherical wave front close to the source. In such situations, if the size of the top cap is smaller than the specimen, the assumption of a planar wave front may lead to error. As long as the waves are sharp and well defined without changing their shape, measurement is fairly accurate [41]. Care should be taken to properly consider the effects.

4.3.1. Impact tests results

Figure 4 presents the results of deformation time-histories for a typical sensor setup of GSs on the side wall of the specimen (sensors set up No. 1) for definition of the first arrival and first peak for direct measurement of V_s and damping ratio under impact loading. Test results for the granular materials, including: V_p, v_{ske}, M, V_s (shear wave velocity), E, v and G of single and two layer materials, are presented in Tables 6 and 7, respectively.

Figure 5 presents the variations of average overall Poisson ratio versus shear wave velocity under isotropic confining pressures of 30, 50 and 80 kPa for whole Dacite and Mudstone materials. Results presented in

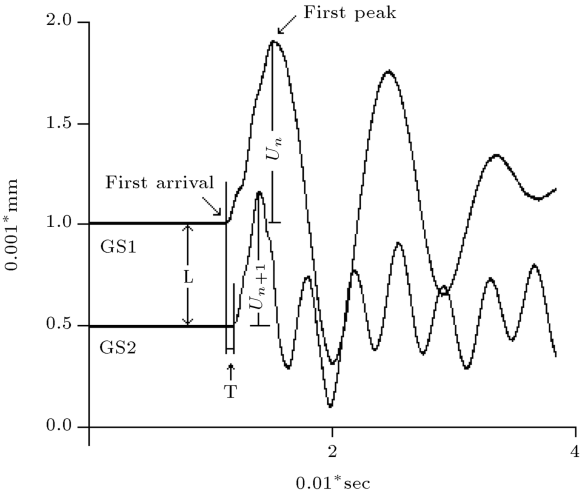

Figure 4. Example of deformation time-history using GSs for setup No. 1 at confining pressure of 80 kPa for definition of first arrival and first peak for direct measurement of V_s and damping ratio under impact loading.

Table 6. Impact tests results for measuring elastic properties of the single material.

Specimen symbol	Material	σ'_3 (kPa)	V_p (m/s)	V_s (m/s)	v_{ske}	M (kPa)	E (kPa)	v	$G_{Hitting}$ (kPa)	$G_{Triaxial}$ (kPa)
D02519GS	Gravel	30	219	129	0.23	68670	60929	0.27	24079	
		50	271	161	0.23	105783	90976	0.23	37093	36695
		80	321	190	0.23	148203	123263	0.19	51967	
	Sand	30	371	193	0.315	214312	141807	0.23	57880	
		50	434	225	0.315	292728	187504	0.19	79058	75894
		80	522	271	0.315	424226	262270	0.14	114572	
M02519GS	Gravel	30	312	183	0.24	97572	85388	0.28	33380	
		50	340	199	0.24	115817	98465	0.24	39622	40239
		80	382	223	0.24	145616	120130	0.21	49816	
	Sand	30	278	164	0.23	77098	70887	0.31	27034	
		50	309	183	0.23	95311	82126	0.23	33421	34590
		80	341	202	0.23	116005	95831	0.18	40677	
D0219	Fresh	30	255	137	0.3	107690	84306	0.37	30769	
		50	318	170	0.3	166477	120815	0.27	47565	47244
		80	387	207	0.3	247453	171096	0.21	70701	
	Reused	30	241	124	0.32	96098	63766	0.25	25438	
		50	292	150	0.32	140803	87301	0.17	37271	36289
		80	367	189	0.32	222396	131630	0.12	58870	
M0219	Fresh	30	313	183	0.24	114976	91425	0.16	39334	
		50	346	203	0.24	141067	110050	0.14	48260	46045
		80	379	222	0.24	169209	129090	0.12	57887	
	Reused	30	266	156	0.24	83334	64716	0.14	28509	
		50	308	180	0.24	111184	83859	0.1	38037	385544
		80	338	198	0.24	134290	99576	0.08	45941	
MD0219	Mudstone	26.7	309	181	0.24	112256	92834	0.21	38403	
		30	315	184	0.24	116532	93290	0.17	39866	
		50	345	202	0.24	139564	109581	0.15	47746	46185
		80	384	224	0.24	172831	133077	0.13	59126	
	Dacite	26.7	230	123	0.3	87080	64700	0.3	24880	
		30	253	135	0.3	105216	76043	0.26	30062	
		50	319	170	0.3	167742	112552	0.17	47926	47691
		80	382	204	0.3	241021	154171	0.12	68863	
DM0219	Dacite	30	257	133	0.32	108659	74538	0.27	29346	
		50	313	163	0.32	162140	106847	0.22	43790	45082
		80	389	202	0.32	249204	163962	0.19	67303	
	Mudstone	30	253	148	0.24	114354	60648	0.18	25633	
		50	319	186	0.24	141519	93081	0.14	40865	39513
		80	382	224	0.24	169619	129891	0.11	58718	
MD0219-fresh	Mudstone	30	315	184	0.24	115054	92645	0.16	39866	
		50	345	202	0.24	142004	107955	0.13	47746	43343
		80	384	224	0.24	170261	130648	0.1	59126	
	Dacite	30	253	135	0.3	105216	78925	0.31	30062	
		50	319	170	0.3	167742	120484	0.26	47926	45745
		80	382	204	0.3	241021	168842	0.23	68863	
STC	Toyoura sand	30	265	133	0.333	110859	67586	0.218	27756	-
		50	359	179	0.333	202509	121755	0.201	50703	50000
		80	416	208	0.333	272459	160633	0.177	68217	-
	Tire chips	30	97	47	0.35	6397	3669	0.243	1476	-
		50	122	59	0.35	10008	5997	0.298	2310	2308
		80	173	83	0.35	20210	12651	0.356	4664	-
STC5050-7030	STC5050	30	264	120	0.37	81169	41538	0.24	16749	-
		50	316	144	037	117067	56473	0.169	24157	23524
		80	362	165	0.37	153865	73872	0.156	31750	-
	STC7030	30	304	140	0.365	134909	69409	0.21	28682	-
		50	326	150	0.365	155050	75981	0.153	32963	32609
		80	367	169	0.365	197191	95444	0.138	41923	-

Table 7. V_p and M values of two layered materials under impact loading.

Specimen symbol	σ_3' (kPa)	V_p (m/s)	M (kPa)
D02519GS	30	299	1336
	50	350	183130
	80	404	244462
M02519GS	30	297	87943
	50	326	106235
	80	356	127091
D0219	30	251	103859
	50	301	149132
	80	373	229387
M0219	30	296	102883
	50	327	125332
	80	359	151247
MD0219	30	269	102490
	50	281	11754
	80	325	149393
DM0219	30	377	200624
	50	281	111528
	80	326	150026
MD0219-fresh	30	386	210100
	50	230	75028
	80	330	153847
STC	30	376	199617
	50	149	25062
	80	177	35393
STC5050-7030	30	213	50858
	50	287	107951
	80	316	130961
	30	362	172085

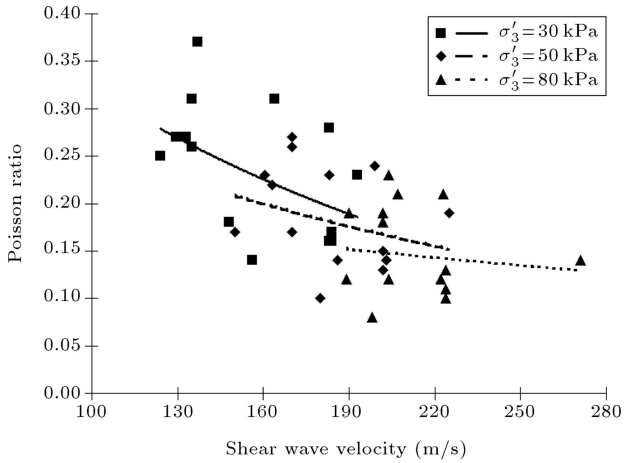

Figure 5. Variations of overall Poisson's ratio versus shear wave velocity at different σ_3' for dacite and mudstone materials.

Figure 5 indicate that the overall Poisson ratio for all materials decreases with increasing confining pressures. The behavior of tire chips is an exception, where the overall Poisson ratio increases as σ_3' increases and follows the range (0.2-0.35) identified by Edeskär [36]. However, the Poisson ratio of tire rubber is 0.5 [42], which means that this material would deform at a constant volume. Moreover, the results presented in Table 5 indicate that v_{ske} of Toyoura sand may be increased by increasing the percentage of tire chips in the mixture.

Generally, the overall Poisson ratio for Toyoura sand, for the confining pressures of 30, 50 and 80 kPa, are 0.218, 0.201 and 0.177, respectively. The overall Poisson ratio for air pluviated Toyoura sand ranges from between 0.15 to 0.2 for σ_v'/σ_h' (σ_v' : vertical stress, σ_h' : horizontal stress), ranging from 0.5 to 2, with an average of 0.17, for isotropic specimen [43]. It is worth noticing that the v_{ske} of Toyoura sand is equal to 0.333, which is comparable to the value of 0.3-0.35 in previous studies [39].

Figure 6(a) and (b) present the shear wave velocity at different confining pressures for Dacite and Mudstone materials. It is found that the shear wave velocity increases with an increase in confining pressure. It is worth noting that, in general, the shear wave velocities of the fresh materials are higher than those of the reused materials. The shear wave velocity of the sand Dacite is two times higher than that of the gravel Dacite. Moreover, the increasing rate of shear wave velocity with confining pressures for Dacite materials is much higher than the same rate for Mudstone materials.

Figure 7 presents shear wave velocity at different confining pressures for STC5050 and STC7030. Similarly, results indicate that the shear wave velocity increases as confining pressure increases. Moreover, results indicate that the shear wave velocity of the STC7030 is generally higher than that of Toyoura sand at a confining pressure of 30 kPa. Thus, it seems that the optimal amount of tire chips in Toyoura sand by mixture weight is around 30%, which is in accordance with previous studies [12]. Moreover, according to Tables 6 and 7, the average M value of the layered specimen (mixture) is close to that of the weaker materials.

Top platen-end specimen interface effects. Figure 8 shows the shear wave velocity ratio (along the top plate-end specimen to only over the specimen) versus confining pressure for mudstone, gravel mudstone and gravel Dacite. Based on results presented in Figure 8, it may be concluded that by increasing the confining pressure to 80 kPa, the interface effect over the measured wave velocity decreases. Moreover, it seems that the particle origin is an influential factor on the shear

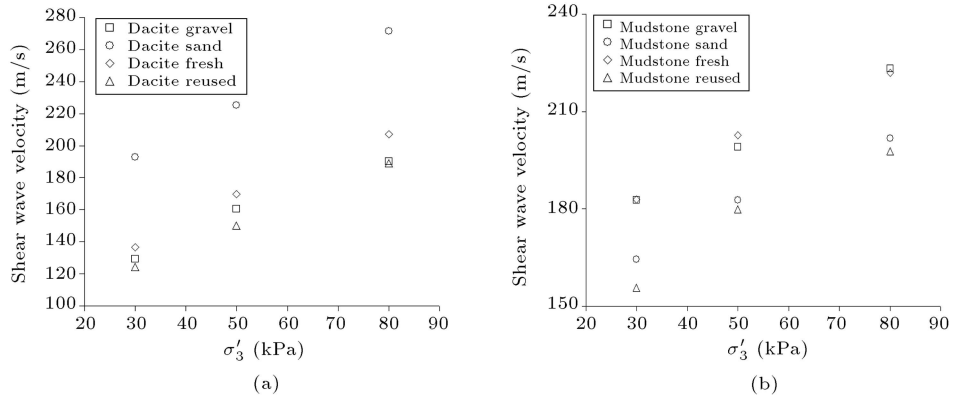

Figure 6. Variation of shear wave velocity versus confining pressure in different materials: (a) Dacite; and (b) mudstone.

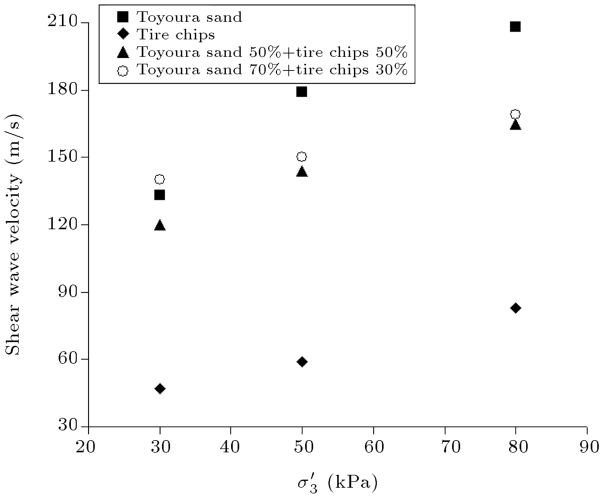

Figure 7. Variation of shear wave velocity versus confining pressure of Toyoura sand, tire chips and their mixtures.

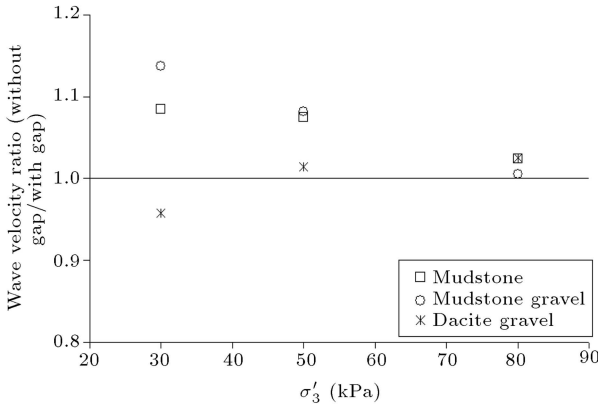

Figure 8. Variation of shear wave velocity ratio versus confining pressure at top platen-end specimen interface.

wave velocity ratio at the interface, so that the effect is negligible for Dacite materials, even at low confining pressure.

Effect of materials interface thickness. Figure 9 shows the shear wave velocity ratio at the interface of

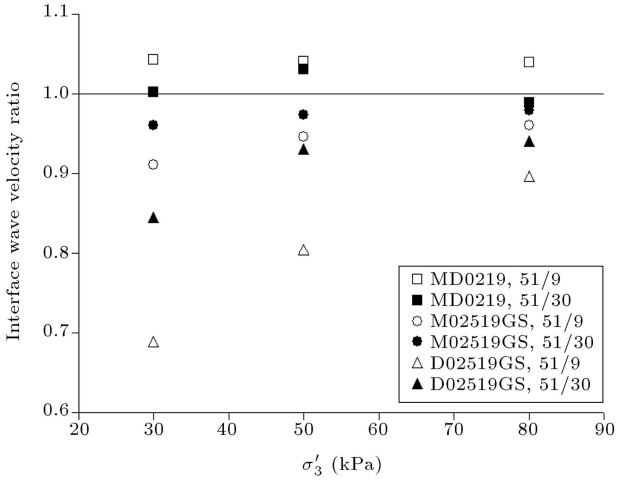

Figure 9. Variation of shear wave velocity ratio versus confining pressure for different interface materials thickness.

two different materials with different thickness versus confining pressure. The numbers in the legend are representative of interface layer thickness in centimeters. As indicated in Figure 9, the shear wave velocity ratio at the interface is dependent on material thickness, as well as the velocity of materials in the upper or lower 30 cm location. The magnitude of wave reflection was low at the material interface owing to high damping. Generally, some reflection is visible only in the ground with two layers at an impedance ratio far from one (< 0.5) [41].

Effect of material location in the upper or lower 30 cm in a specimen. Material location in the upper or lower 30 cm in a specimen has a visible influence on measured shear wave velocity, especially for mudstone materials, at low to medium confining pressures. However, its importance may decrease at a confining pressure of 80 kPa (Figure 10).

Membrane effects over measured wave velocity. Considering a density of 10 kN/m^3 for the membrane,

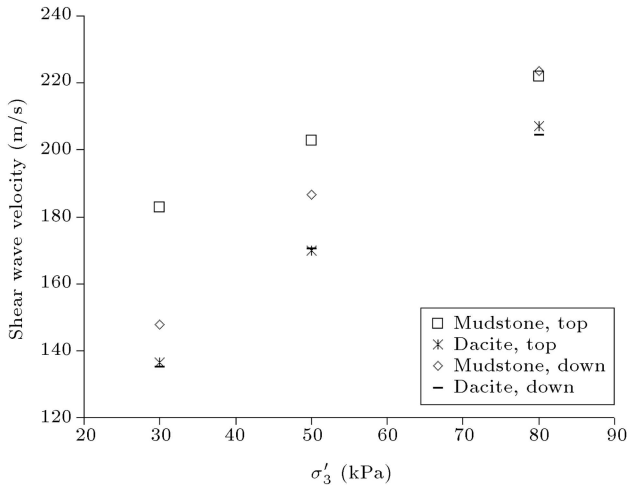

Figure 10. Effect of material location over shear wave velocity versus confining pressure.

the values of V_p and V_s are around 27 m/s and 9 m/s, respectively. Moreover, due to complete contact between the specimen and membrane, its negligible effect over the measured wave velocity was ignored.

4.4. Cyclic triaxial testing program

Nine cyclic triaxial tests were carried out in this research on granular materials, according to ASTM D3999 [37] (Table 4). As mentioned before, to save cost and time, the cyclic tests were performed on the same specimens after impulse loading. The specimens were subjected to an isotropic confining pressure of 5 kPa. Then, they were loaded under initial isotropic conditions ($k_c = \sigma'_1/\sigma'_3 = 1$) or initial anisotropic conditions ($k_c = 2$). During the test, the amount of anisotropy coefficient was fixed by applying the desired loads from the load cell of the triaxial equipment. Forty cycles of sinusoidal loading were applied at a very small strain level. Test results for cycles 1 to 40 have been recorded. This procedure was then repeated at higher strain levels (about twice the initial amplitude) until the maximum strain level was achieved. Axial loads, total vertical deformation and local horizontal-vertical deformations, were measured at periodic intervals. The sampling frequency was at least 50 data points per cycle (according to ASTM D3999 [37], minimum sampling rate should be 40 data points per cycle). Cyclic tests were performed under stress-control conditions.

4.4.1. Cyclic test results

Tests results, including Young's modulus (E) and damping ratio (D) versus axial strains (ε_1), have been calculated based on the stress-strain hysteresis loop for the 10th cycle, according to ASTM D3999 [37].

Young modulus. E versus ε_1 data points under a confining pressure of 50 kPa are shown in Figure 11. It can be seen that E is strongly dependent on the axial strain. At low strain amplitudes, the modulus is nearly constant, at its highest value, $E_{\max}$, but decreases while strain amplitude is increasing. The extrapolation method was employed from 0.0001% strain to obtain $E_{\max}$ (or $G_{\max}$ by overall Poisson ratio) and the results are compared with the wave velocity results using GSs. Reasonable agreement was observed between the modulus of the cyclic triaxial and that of wave velocity. Generally, the value of the shear modulus evaluated from the wave velocity is slightly higher than that of the cyclic triaxial using GSs (Table 6). Moreover, in the anisotropic initial stress condition for the sand and gravel Mudstone, a higher amount of E is obtained (Figure 11(a) and (h)). This is because, at higher values of anisotropy state, the amount of initial $\sigma'_m = (\sigma'_1+2\sigma'_3)/3$ increases, and this is the main reason for the increase of E.

It can be seen that there is good agreement between the results of GSs and LDTs for local strain measurements under low speeds of loading. Moreover, test results indicate that there is a slight discrepancy in the E value using LDTs at small strain levels in some specimens.

Tests results, including E versus ε_1 under confining pressure of 50 kPa, using GSs and LDTs for measuring the local strains of Toyoura sand, tire chips, and STC5050 and STC7030 materials, are shown in Figure 12. Generally, the modulus decreases as the tire chips continue increasing [14]. Soil-tire chip mixtures exhibit lower small-strain stiffness as the percentage of tire chips increases in the mixture. This is mainly due to the negligible contribution of the soft tire chip solids on the stiffness of the soil-tire chips solid skeleton. The results presented in Figure 12 indicate that $E_{\max}$ was estimated to be around 120000 kPa (using the extrapolation method) for Toyoura sand, which is in accordance with previous studies [44]. Then, by assuming the overall Poisson ratio to be equal to 0.2, the shear modulus was estimated at around 50000 kPa, which is comparable with 50600 kPa using the wave velocity method (Table 6).

Damping ratio. Figure 13 presents D versus ε_1 data points at the 10th cycle for materials tested at a confining pressure of 50 kPa. The damping ratio decreases as increases. Similar to the case of E, there is good agreement between the results of GS and LDT for the damping ratio (Figure 13). Generally, it can be seen that under the anisotropic initial stress condition for the lightweight sand and gravel Mudstone, a higher amount of damping ratio is obtained at the studied confining pressure (Figure 13(a) and (h)).

Figure 14 shows versus data points for Toyoura sand, tire chips, and STC5050 and STC7030 at a confining pressure of 50 kPa, using a large cyclic triaxial test. Generally, the inclusion of tire chips

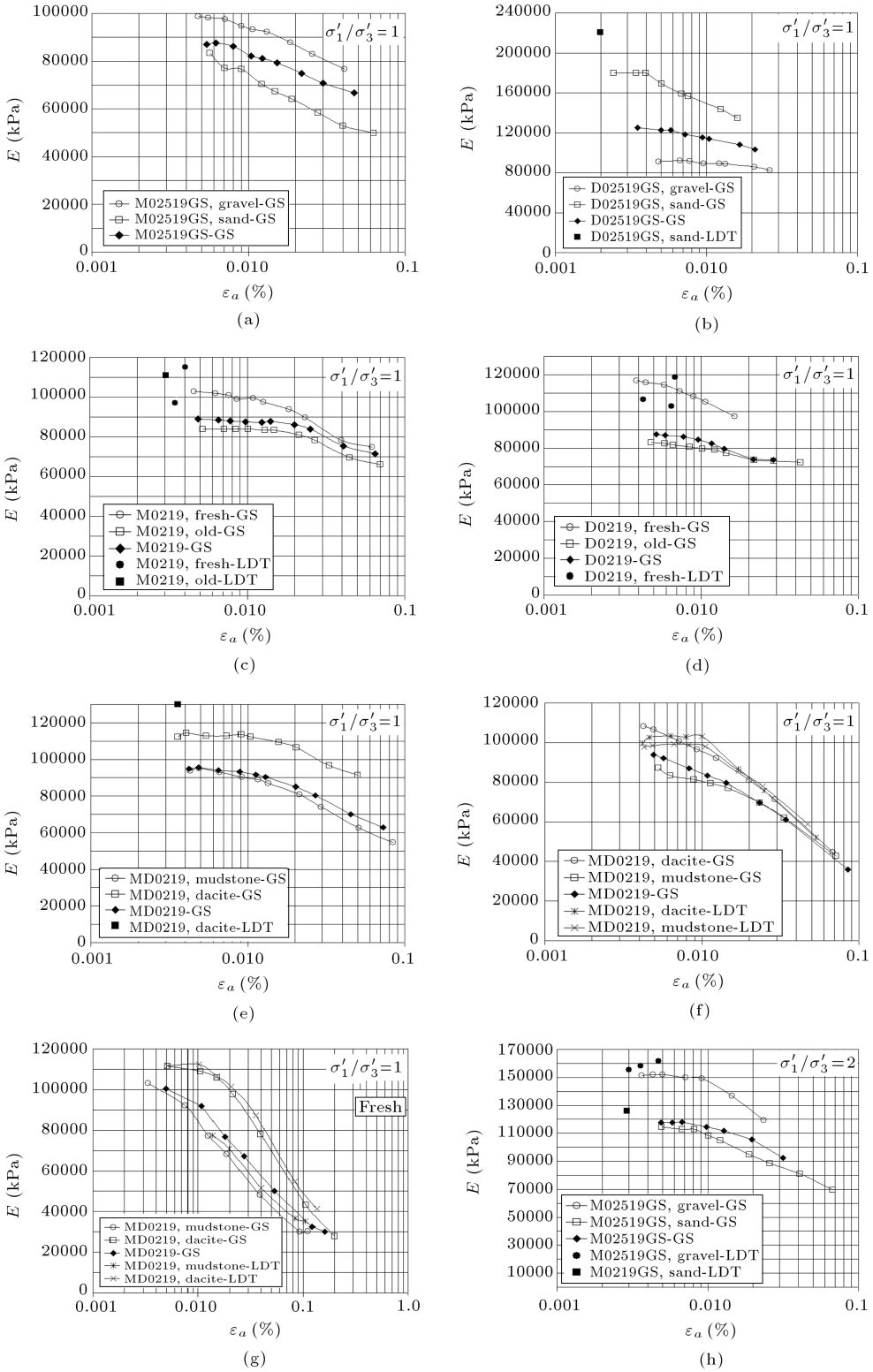

Figure 11. Variation of E versus γ using large cyclic triaxial tests for different materials at $\sigma'_3 = 50$ kPa.

in Toyoura sand leads to an increase in the damping ratio properties of the mixture in comparison to pure sand. This is due to the deformability of rubber particles, as well as to the interaction of soil rubber particles, which are materials having significantly different elastic and thermal properties. Finally, E and D results indicate that the optimum amount of tire chip contained in Toyoura sand is around 30% by weight. Previous studies [14] have indicated that for a contained amount of tire chip by mixture weight below

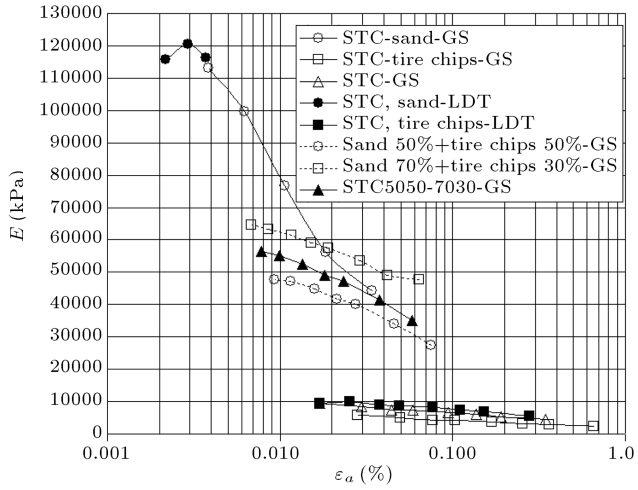

Figure 12. Variation of E versus γ using large cyclic triaxial tests for Toyoura sand, Tire Chips, STC5050 and STC7030 at $\sigma_3' = 50$ kPa.

30-40% and confining pressure lower than 300 kPa, the mixtures exhibit high shear strength, satisfactory compaction characteristics and dilatant behavior, and the response of the mixtures is characterized as sand-like.

4.5. Damping behavior under impact loading

The amplitude of forced vibration responses (stress waves and induced shear strains) in real materials attenuate with distance, mainly due to material and radiation (or geometric) damping. According to Wolf [45], in the case of shallow layers of soil, radiation damping can be drastically reduced and material damping is the primary source. Moreover, the obtained results of Soil-Structure Interaction (SSI) analysis lead to an indirect assessment of the importance of energy dissipation due to soil material damping compared with dissipation due to radiation damping [46]. However, radiation damping in SSI analysis could be significant in some cases, leading, at times, to effective values of damping in the first mode of 20% or 25% under horizontal excitation and up to 50% or more in vertical vibration [47]. This, however, is not the case for triaxial tests with a rigid cap having a constant area under longitudinal impact loading (i.e. one dimensional longitudinal wave propagating in a rod), where the effects of material damping often dominate those of geometric damping. Moreover, due to the confining pressure effect in these layered triaxial specimens, the impedance ratio will be different from, but close to, one. Hence, the amount of reflection, and, as a result, geometric damping may be negligible [41].

Similar to the equation of motion for damped free vibration in a system of single degrees of freedom, the logarithmic decrement of deformations for forced vibration between two distances is defined by:

$$\delta = \log_e \left(\frac{U_n}{U_{n+1}} \right), \tag{6}$$

where, U_n and U_{n+1} are the first peak wave amplitudes in two successive locations, n and $n+1$, respectively. From the above equation, average damping ratio can be deduced as:

$$D_{av} = \frac{\delta}{\sqrt{4\pi^2 + \delta^2}}. \tag{7}$$

From the deformation time-histories recorded by GSs and using the reduced amplitude technique at different levels of triaxial specimen under impact loading, damping ratio is calculated, and also presented in Figures 13 and 14. Generally, damping ratio, using the amplitude decay method, is higher than that of cyclic triaxial tests, due to the high speed of loading [7]. Moreover, the STC7030 has the highest D in the amplitude decay method by impact loading.

Figure 15 presents the average damping ratio versus isotropic confining pressure for mudstone and Dacite using the amplitude decay method. The variations of D with confining pressures for the mudstone materials are less pronounced and almost constant, whereas the variations for the Dacite materials are more and decrease moderately. In general, the D value, using the amplitude decay method for the mudstone material at low strain, is higher than that of the Dacite material.

Table 8 presents the damping ratio results using the amplitude decay method by hitting at a confining pressure of 50 kPa for the layered large triaxial specimen. Generally, the damping ratio for the layered specimen is higher than that of the single material in the upper or lower 30 cm.

4.6. Particle breakage

Breakage of particles was observed during the triaxial tests. The breakage is usually expressed quantitatively by the Breakage Index, B_g [48]. The value of B_g is

Table 8. D results for different layered specimens using amplitude decay method using impact loading at $\sigma_3' = 50$ kPa.

Material symbol	D (%)
M02519GS	4.40
D02519GS	4.06
M0219	6.38
D0219	3.83
MD0219	4.74
DM0219	6.50
MD0219-fresh	5.90
STC	7.31
STC5050-7030	11.42

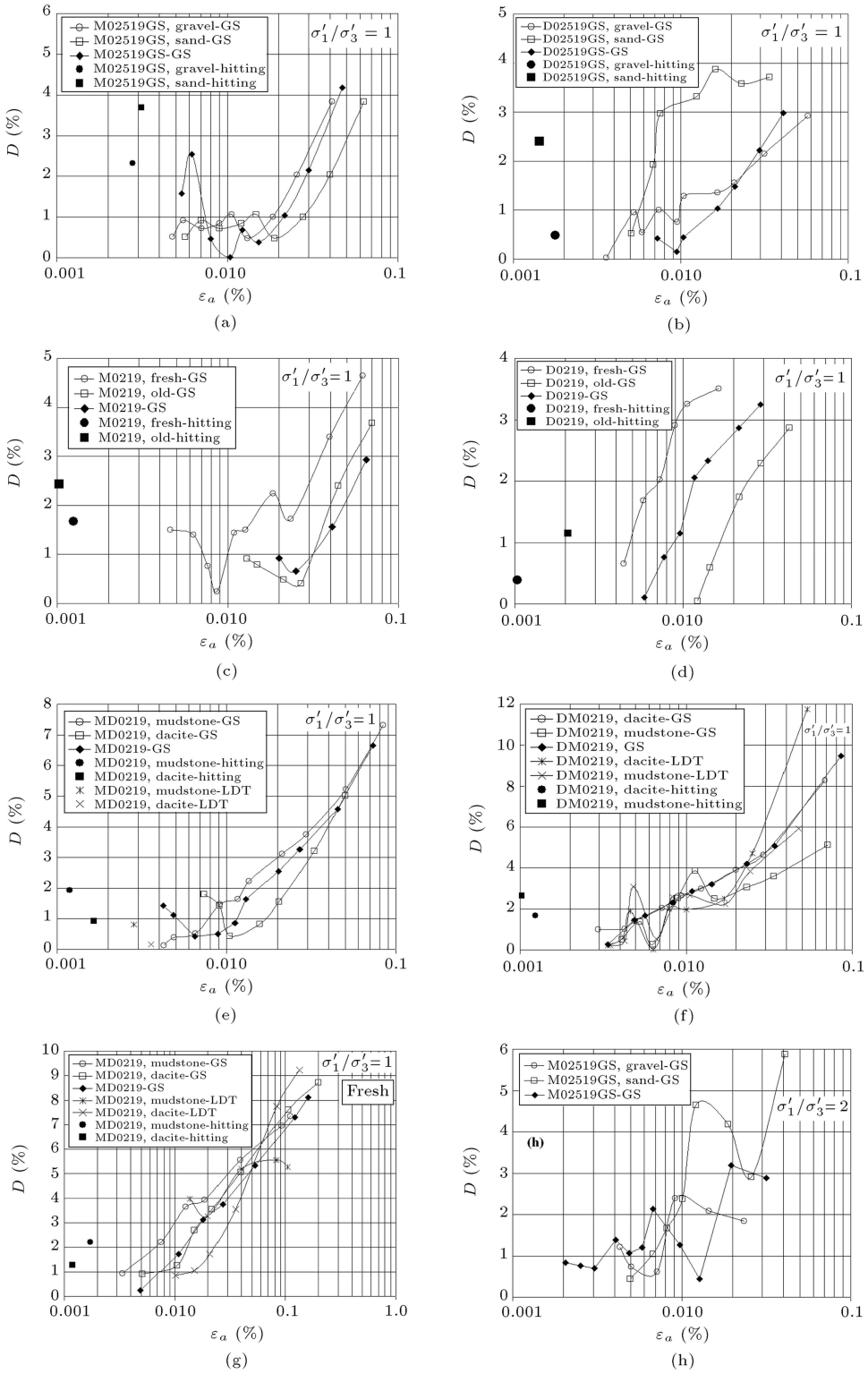

Figure 13. Variation of D versus γ using large cyclic triaxial tests and amplitude decay method for different materials at $\sigma'_3 = 50$ kPa.

calculated by sieving the sample using a set of sieves (19 to 0.25 mm) before and after testing. The percentage of particles retained in each sieve is determined at both stages. Due to the breakage of the particles, the percentage of particles retained on the large size sieves will decrease and the percentage of particles retained on the smaller size sieves will increase. The sum of the decreases will be equal to the sum of the increases in the percentage retained. The decrease (or increase) is the value of the breakage factor, B_g. Table 9 presents the

Table 9. Marsal breakage index at confining pressure of 50 kPa.

Material	B_g (%) after compaction	B_g (%) after cyclic test	B_g (%) after monotonic test
M02519GS-gravel	3.88	4.20	NIA
M02519GS-sand	2.45	3.58	NIA
D02519GS-gravel	2.04	4.04	NIA
D02519GS-sand	0.78	0.93	NIA
M0219-fresh	2.98	3.13	NIA
M0219-reused	1.47	3.36	NIA
D0219-fresh	0.98	3.47	NIA
D0219-reused	0.60	0.92	NIA
Mudstone-MD0219	2.71	3.06	NIA
MD0219-Dacite	0.95	2.00	NIA
MD0219-Mudstone-fresh	NIA	3.06	NIA
MD0219-Dacite-fresh	NIA	0.95	NIA
MONO-MD0219-Mudstone	2.65	NIA	4.13
MONO-MD0219-Dacite	1.22	NIA	2.72
MONO-D02519GS-gravel	NIA	NIA	3.12
MONO-D02519GS-sand	NIA	NIA	1.26
MONO-M02519GS-gravel	NIA	NIA	6.99
MONO-M02519GS-sand	NIA	NIA	3.31

NIA: Not Information Available.

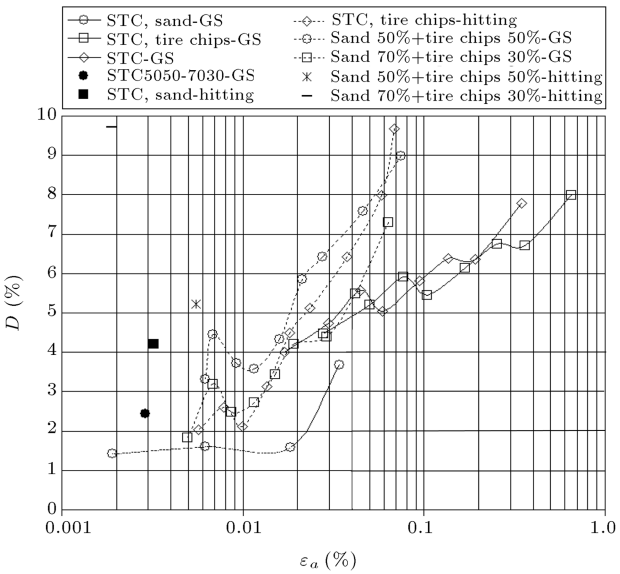

Figure 14. Variation of D versus γ using large cyclic triaxial tests and amplitude decay method for Toyoura sand, tire chips, STC5050 and STC7030 materials at $\sigma'_3 = 50$ kPa.

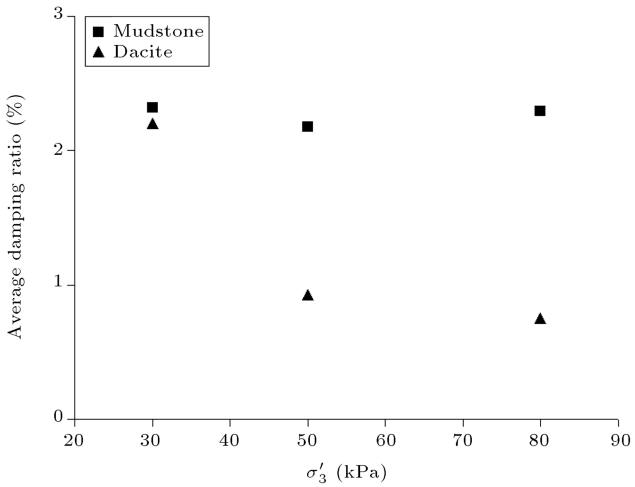

Figure 15. Average damping ratio versus confining pressure for Mudstone and Dacite using amplitude decay method.

results of the Marsal Breakage Index, B_g, for the tested materials after compaction, and monotonic and cyclic tests. A considerable amount of B_g is related to the breakage of the particle at the specimen construction stage (B_g=2.19%).

Results show that particles more susceptible to breakage materials (mudstone in comparison to Dacite) have higher damping ratio. Moreover, B_g for gravel is higher than that of the sand and mixed sand-gravel materials. This may be due to the increase of stress concentration at particle contacts. In comparison to static tests (B_g=3.59%), the average value of B_g in cyclic loading (3.23%) decreases. It seems that B_g does not have considerable value in cyclic tests and is moderately dependent on the strain level applied. Therefore, the values of B_g are less dependent on the

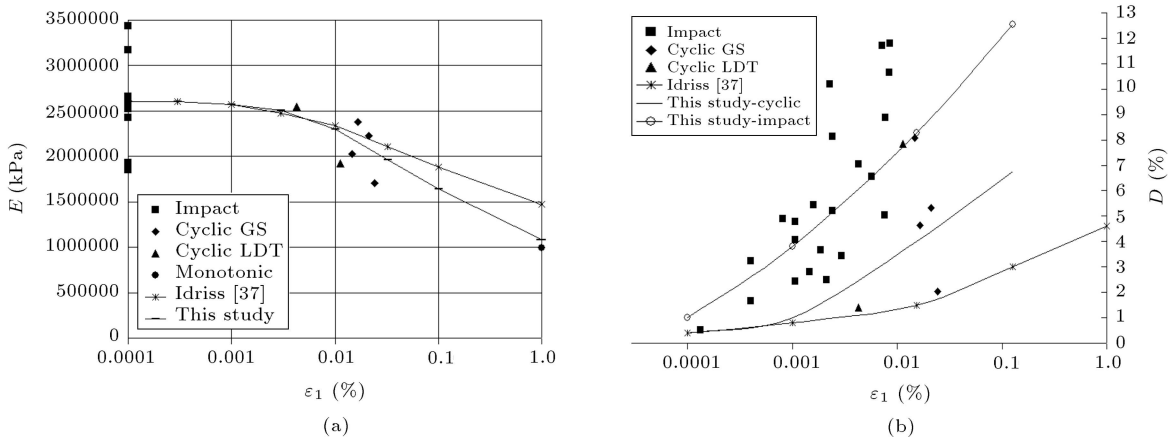

Figure 16. (a) $E-\gamma$, and (b) $D-\gamma$ of Mudstone rock specimen.

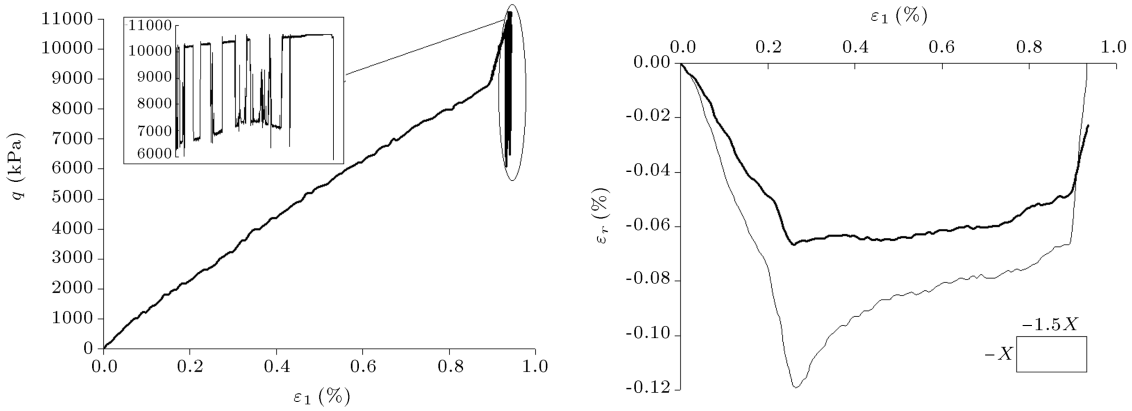

Figure 17. Stress-radial strain-axial strain behavior of mudstone rock specimen under uniaxial compression test.

type of loading, and most dependent on the imposed strain level at low confining pressures.

4.7. Behaviors of mudstone rock specimen

Wave velocity, damping, and cyclic and monotonic behaviors of a mudstone rock specimen under uniaxial, without using a membrane, is studied using small triaxial equipment. The average uniaxial strength of the specimens is around 9900 kPa. Similar to the granular materials, using impulse loading, the average value of V_p for the intact mudstone rock specimen is 1088 m/s (i.e. E=2606578 kPa) (Figure 16(a)). In the rock specimen with a visible crack, the average value of V_p in the fractured zone is about 333 m/s, with an average of 495 m/s for the whole specimen. Cyclic uniaxial testing is carried out under initial deviator stress smaller than 10% uniaxial strength (775 kPa) and cyclic stress ratio of around 0.38. Both LDT and GS were used for measuring the local strains, and the values at 0.01% axial strain are about 2233035 and 2082587 kPa, respectively. These results are in good agreement with velocity results. Using the amplitude decay method under impact loading, the average damping ratio of the rock specimen is calculated and shown in Figure 16(b). The damping ratios in cyclic loading are also shown in Figure 16, which is half of the impact loading. Figure 17 shows the stress-radial strain-axial strain behavior of mudstone rock specimens under uniaxial testing. The secant modulus (E_{50}) and Poisson ratio (v_{50}) are about 990000 kPa and 0.25, respectively [49]. Using GS, it is possible to record the variation of stress-strain of the rock specimen before the failure state. A significant reduction (about 40%) in the maximum uniaxial compression strength of the rock specimen before failure is observed.

5. Conclusions

In this paper, the feasibility of using high frequency GSs for measuring wave velocity, damping, axial-radial strains under impact, and monotonic and cyclic loadings is investigated. Tests were performed on triaxial specimens of Toyoura sand, tire chips, soil-rubber mixtures, granular mudstone and Dacite, as well as the uniaxial specimen of Mudstone rock. The main results can be summarized as follows:

- For spacing higher than 550 mm between the GSs transducers, determination of the travel time of the first arrival of the compressional wave may be

difficult, due to both near-field and side-reflected waves.

- Generally, increasing confining pressure causes an increase in wave velocity and a decrease in Poisson ratio in granular soil materials. However, in tire chips, increasing confining pressure causes an increase in Poisson ratio.
- The rate of increase in shear wave velocity with confining pressure for Dacite specimens is higher than that of the light-weight mudstone material.
- The shear wave velocity of fresh angular material is higher than that of reused material.
- In the fresh Dacite material, increase in particle size causes a decrease in shear modulus. But, in lightweight mudstone material, increase in particle size causes an increase in shear modulus.
- Materials more susceptible to breakage (i.e. mudstone in comparison to Dacite) have higher damping ratio.
- Tests results indicate that factors such as maximum particle size, grain size distribution, origin of particle, layer thickness at the interface, and the place of the material in the layered specimen influence the trends and variations of wave velocity and damping ratio with confining pressure.
- Using the amplitude decay method for calculating damping ratio at different elevations in the side of the specimens using GSs is one of the new initiatives of this research.
- Using GSs, there is good agreement between the measured shear modulus and damping ratio using cyclic triaxial tests equipped by local measuring systems (e.g. LDTs and GSs) and the results of this study, indicating the reliability of the GSs results.
- Based on the tests results, the optimum percentage of tire chips in Toyoura sand is about 30% by mixture weight. Generally, including rubber in the mixture leads to more pronounced damping properties in comparison to pure Toyoura sand.
- The average constraint modulus for the layered soil specimen is closer to that of the weaker materials.
- GS is a reliable transducer for studying wave velocity and the damping behavior of rock specimens under uniaxial stress conditions.

Acknowledgment

Laboratory tests for this study were carried out during research work conducted by the first author at the Geotechnical Laboratory in the Department of Civil Engineering at the University of Tokyo, Japan. The analytical part of the research was partially supported, financially, by BHRC under grant 90-39-8128(2010), as well as by the National Elite Foundation under grant 15/29016 (2011). The first author is grateful to Professor Ikuo Towhata for this research opportunity, as well as for the valuable comments and discussions on this study. The first author is also thankful for the technical help and assistance provided by respected colleagues at the Geotechnical Laboratory at the University of Tokyo, as well as the Geotechnical Division of BHRC.

References

1. Kim, T.H., Kim, T.H. and Kang, G.C. "Performance evaluation of road embankment constructed using lightweight soils on an unimproved soft soil layer", *Engineering Geology*, **160**, pp.34-43 (2013).
2. Anastasiadis, A., Senetakis, K. and Pitilakis, K. "Small-strain shear modulus and damping ratio of sand-rubber and gravel-rubber mixtures", *Geotechnical and Geological Engineering*, Springer, **30**(2), pp.363-382 (2012).
3. Kaneko, T., Orense, R.P., Hyodo, M. and Yoshimoto, N. "Seismic response characteristics of saturated sand deposits mixed with tire chips", *Journal of Geotechnical and Geoenvironmental Engineering*, **139**(4), pp. 633-643 (2013).
4. Seed, H.B., Wong, R.T., Idriss, I.M. and Tokimatsu, K. "Moduli and damping factors for dynamic analyses of cohesionless soils", *J. Geotech. Eng.*, **112**(11), pp. 1016-1032 (1986).
5. Ham, A., Wang, J. and Stammer, J.G. "Relationships between particle shape characteristics and macroscopic damping in dry sands", *Journal of Geotechnical and Geoenvironmental Engineering*, **138**(8), pp. 1002-1011 (2012).
6. Aghaei Araei, A., Razeghi, H.R., Tabatabaei, S.H. and Ghalandarzadeh, "A. dynamic properties of gravelly materials", *Scientia Iranica*, **17**(4), pp. 245-261 (2010).
7. Aghaei Araei, A., Razeghi, H.R., Tabatabaei, S.H. and Ghalandarzadeh, A. "Loading frequency effect on stiffness, damping and cyclic strength of modeled rockfill materials", *Soil Dynamics and Earthquake Engineering*, **33**, pp. 1-18 (2012).
8. Aghaei Araei, A. "Feasibility study for installation of equipment for measurement maximum shear modulus (high frequency GAP-SENSOR) on large diameter triaxial apparatus for sand and tire chips", *Research Project, National Elite Foundation*, grant no. 15/18192 (2010), under supervision of BHRC (2012).
9. Aghaei Araei, A. "Assessment of the GAP-SENSOR use for measuring maximum shear modulus in layered granular and gravelly materials", *Research Project*, no. 90-39-8128(2010), BHRC, Iran (2013).
10. Aghaei Araei, A., Razeghi, H.R., Tabatabaei, S.H. and

Ghalandarzadeh, A. "Effects of loading rate and initial stress state on stress-strain behavior of rockfill materials under monotonic and cyclic loading conditions", *Scientia Iranica*, **19**(5), pp. 1220-1235 (2012).

11. Yang, J. and Gu, X.Q. "Shear stiffness of granular material at small strains: does it depend on grain size?", *Geotechnique*, **63**(2), pp. 165-179 (2013).
12. Zornberg, J.G., Cabral, A.R. and Viratjandr, C. "Behaviour of tyre shred-sand mixtures", *Canadian Geotechnical Journal*, **41**, pp. 227-241 (2004).
13. Balachowski, L. and Gotteland, P. "Characteristics of tyre chips-sand mixtures from triaxial tests", *Archives of Hydro-Engineering and Environmental Mechanics*, **54**(1), pp. 25-36 (2007).
14. Nakhaei, A., Marandi, S.M., Sani Kermani, S. and Bagheripour, M.H. "Dynamic properties of granular soils mixed with granulated rubber", *Soil Dynamics and Earthquake Engineering*, **43**, pp. 133-138 (2012).
15. Khan, Z.H., Cascante, G. and El Naggar, M.H. "Evaluation of the first mode of vibration and base fixidity in resonant-column testing", *Geotechnical Testing Journal, ASTM*, **31**(1), pp. 65-75 (2008).
16. ASTM D4015. "Standard test methods for modulus and damping of soils by the Resonant-Column method", Re-approved 2000 (1992).
17. Clayton, C.R.I., Priest, J.A., Bui, M., Zervos, A. and Kim, S.G. "The Stokoe resonant column apparatus: Effects of stiffness, mass and specimen fixity", *Geotechnique*, **59**(5), pp. 429-437 (2009).
18. Tallavo, F., Cascante, G. and Pandey, M.D. "Ultrasonic transducers characterization for evaluation of stiff geomaterials", *Géotechnique*, **61**(6), pp. 501-510 (2011).
19. Yang, Y., Cascante, G. and Polak, M.A. "New method for the evaluation of material damping using the wavelet transform", *Journal of Geotechnical and Geoenvironmental Engineering*, **137**(8), pp. 798-808 (2011).
20. Nefeslioglu, H.A. "Evaluation of geo-mechanical properties of very weak and weak rock materials by using non-destructive techniques: Ultrasonic pulse velocity measurements and reflectance spectroscopy", *Engineering Geology*, **160**, pp. 8-20 (2013).
21. Alramahi, B., Alshibli, K.A., Fratta, D. and Trautwein, S. "A suction-control apparatus for the measurement of P and S-wave velocity in soils", *Geotechnical Testing Journal, ASTM*, **31**(1), pp. 12-23 (2008).
22. Youn, J.U., Choo, Y.W. and Kim, D.S. "Measurement of small-strain shear modulus Gmax of dry and saturated sands by bender element, resonant column, and torsional shear tests", *Canadian Geotechnical Journal*, **45**(10), pp. 1426-1438 (2008).
23. Fratta, D. and Santamarina, J.C. "Waveguide device for multi-mode, wideband testing of wave propagation in soils", *Geotechnical Testing Journal*, **19**, pp. 130-140 (1996).
24. Goto, S., Tatsuoka, F., Shibuya, S., Kim, Y.S. and Sato, T. "A simple gauge for local strain measurements in the laboratory", *Soils and Foundations*, **31**(1), pp. 169-180 (1991).
25. Tatsuoka, F., Teachavorasinskun, S., Dong, J., Kohata, Y. and Sato, T. "Importance of measuring local strains in cyclic triaxial tests on granular materials", *Proc. ASTM symposium dynamic geotechnical testing II, ASTM*, STP 1213, pp. 288-302 (1994).
26. Tatsuoka, F., Modoni, G., Jiang, G.L., Anh Dan, L.Q., Flora, A., Matsushita, M. and Koseki, J. "Stress-strain behavior at small strains of unbound granular materials and its laboratory tests", Keynote lecture, proc. workshop on modeling and advanced testing for unbound granular materials, January 21 and 22, Lisboa (Ed. by A.G Correia), Balkema, pp. 17-61 (1999).
27. Scholey, G.K., Frost, J.D., Lo Presti D.C.F. and Jamiolkowski, M. "A review of instrumentation for measuring small strains during triaxial testing of soil specimens", *Geotechnical Testing Journal*, **18**(2), pp. 137-156 (1995).
28. Rashidian, M., Ishihara, K., Kokusho, T., Kanatani, M. and Toshiro, O. "Undrained shearing behavior of very loose gravelly soils", *Static and Dynamic Properties of Gravelly Soils*, Geotechnical Special Publication No. 56, pp. 77-91 (1995).
29. Kokusho, T. "Cyclic triaxial test of dynamic soil properties for wide strain range", *Soils and Foundations*, **20**, pp. 45-60 (1980).
30. Hoque, E. and Tatsuoka, F. "Triaxial system measuring loading-rate effects of sand deformation in cycle", *Geotechnical Testing Journal, ASTM*, **27**(5), pp. 483-495 (2004).
31. Santucci de Magistris, F., Koseki, J., Amaya, M., Hamaya, T., Sato, T. and Tatsuoka, F. "A triaxial testing system to evaluate stress-strain behavior of soils for wide range of strain and strain rate", *Geotechnical Testing Journal*, **22**(1), pp. 44-60 (1999).
32. ASTM D6270 "Standard practice for use of scrap tyres in civil engineering applications" (1998).
33. ASTM C127 "Test method for density, relative density (specific gravity), and absorption of coarse aggregate" (2012).
34. ASTM D698 "Standard test methods for laboratory compaction characteristics of soil using standard effort (600 kN-m/m^3)" (2007).
35. Edeskar, T. "Use of tyre shreds in civil engineering applications-Technical and environmental properties", PhD Dissertation, Lulea University of Technology, Department of Civil and Environmental Engineering, Division of Mining and Geotechnical Engineering, Sweden (2004).

36. ASTM C535 "Standard test method for resistance to degradation of large-size coarse aggregate by abrasion and impact in the Los Angeles machine" (2012).

37. ASTM D3999 "Standard test methods for the determination of the modulus and damping properties of soils using the cyclic triaxial apparatus" (2006).

38. ASTM D4767 "Standard Test Method for consolidated undrained triaxial compression test for cohesive soils" (2004).

39. Ishihara, K. and Tsukamoto, Y. "Cyclic strength of imperfectly saturated sands and analysis of liquefaction", *Proc. Japan Acad. Ser. B*, **80**, pp. 372-391 (2004).

40. Santamarina, J.C., Klein, K.A. and Fam, M.A. "Soils and Waves: Particulate Materials Behavior, Characterization and Process Monitoring", New York, Johan Wiley&Sons, USA (2001).

41. Sundarraj, K.P. "Evaluation of deformation characteristics of 1-G model ground during shaking using a Laminar Box", PhD dissertation, University of Tokyo, Japan (1996).

42. Beatty, J.R. "Physical properties of rubber compounds: Mechanics of Pneumatic Tires", S.K. Clark, ed., United States Department of Transportation, National Highway Traffic Administration, Washington, D.C. (1981).

43. Hoque, E. and Tatsuoka, F. "Anisotropy in elastic deformation of granular materials", *Soils and Foundations*, **38**(1), pp. 163-179 (1998).

44. Builes, M., Garcıa, E. and Riveros, C.A. "Dynamic and static measurements of small strain moduli of Toyoura sand", *Rev. Fac. Ing. Univ. Antioquia, Marzo*, **43**, pp. 86-101 (2008).

45. Wolf, J.P. "Soil-structure interaction analysis in time domain", Prentice-Hall, Englewood, Cliffs, NJ. 446 p (1988).

46. Ambrosini, R.D. "Material damping vs. radiation damping in soil-structure interaction analysis", *Computers and Geotechnics*, **33**(2), pp. 86-92 (2006).

47. Ostadan, F., Deng, N. and Roesset, J.M. "Estimating total system damping for soil-structure interaction systems", *Proceedings Third UJNR Workshop on Soil-Structure Interaction*, March 29-30, Menlo Park, California, USA (2004).

48. Marsal, R.J. "Large scale testing of rockfill materials", *Journal of the Soil Mechanics and Foundations Division, ASCE*, **93**, SM2, pp. 27-43 (1967).

49. Hayano, K., Sato, T. and Tatsuoka, F. "Deformation characteristics of a sedimentary soft mudstone from triaxial compression tests using rectangular prism specimens", *Geotechnique*, **47**(3), pp. 439-449 (1997).

Biographies

Ata Aghaei Araei received his PhD degree from Iran University of Science and Technology (IUST), Iran, in 2011. He was PhD researcher in the Geotechnical Laboratory of Civil Engineering at the University of Tokyo, Japan. He is Faculty Member of the Road, Housing and Urban Development Research Center (BHRC), Iran, where he is working as Senior Geotechnical Engineer and Head of the Geotechnical Laboratory. His primary research interests include monotonic and dynamic testing on geomaterials, microzonation, and geotechnical equipment construction.

Ikuo Towhata graduated from the Civil Engineering Department of the University of Tokyo in 1977 and obtained his Doctoral Degree from the same department. He worked at the University of British Columbia, Canada, as Post-Doctoral fellow, and at the Asian Institute of Technology, Thailand, as Assistant Professor. He has been Professor of Geotechnical Engineering at the University of Tokyo since 1994.

His research interests lie in the fields of geotechnical earthquake engineering, mitigation of damage caused by rainfall-induced slope failure, microscopic observation of soil behavior and others.

His research methodology consists of damage reconnaissance, model tests associated with triaxial and torsion shear tests and analytical solution. He has authored a book published by Springer Verlag in 2008, entitled: "Geotechnical Earthquake Engineering". He is currently Vice President of the International Society of Soil Mechanics and Geotechnical Engineering for Asia and President of the Japanese Geotechnical Society.

Hamid Reza Rezeghi received his PhD degree from Tohoku University, Japan, in 2000, and is now Associate Professor in the School of Civil Engineering at Iran University of Science and Technology, Iran. His research interests include geotechnical and geoenvironmental engineering.

Saeid Hashemi Tabatabaei received his PhD degree from Roorkee University, India, in 1992, and is currently Associate Professor at the Building and Housing Research Center (BHRC), Iran, where he is Head of the Geotechnical Department. He has over 21 years experience in the field of geotechnical engineering, and has been involved in over 40 engineering projects in the fields of landslide hazard and risk assessment, slope stability analysis and mitigation, soil improvement, geological mapping for microzonation of rural areas, and site investigation.